# Application of Pulsed-Gradient Fourier Transform Nuclear Magnetic Resonance to the Study of Self-Diffusion of Phospholipid Vesicles†

George G. McDonald* and J. M. Vanderkooi

ABSTRACT: A pulsed-gradient Fourier transform nuclear magnetic resonance (NMR) technique was applied to the study of diffusion of phospholipid vesicles. The diffusion coefficient of dimyristoyllecithin vesicles (DML) in a $D_2O$–phosphate buffer at 37° is $D = 1.9 \times 10^{-6}$ cm$^2$/sec. In a solution made viscous by DNA addition, the diffusion coefficient of DML vesicles was $3.5 \times 10^{-7}$ cm$^2$/sec. These values compare favorably with the diffusion rate for liposomes as determined by ultracentrifugation and by Stokes law calculation. The data suggest that DML diffusion is controlled primarily by whole liposome migration as opposed to movement of individual molecules within the liposome, liposome rotation, or fast exchange between lecithin molecules in solution and in vesicles.

Phospholipid vesicles prepared by sonication provide a model system for biological membranes which is advantageous in several ways. First, they resemble biological membranes in that they are composed of a single bilayer of phospholipids. Secondly, they can be prepared in large quantities with a high degree of size homogeneity. Consequently, a great deal of attention has been focused upon the physical characteristics of phospholipid vesicles, with respect to their size (Huang, 1969; Huang and Lee, 1973), the lateral diffusion of individual phospholipids in the bilayer (Lee et al., 1973) as well as $T_1$ and $T_2$ relaxation (Horwitz et al., 1973; McLaughlin et al., 1973).

In the work described here, the diffusional properties of dimyristoyllecithin vesicles were measured using a pulsed-gradient Fourier transform nuclear magnetic resonance (NMR)[1] technique. The results are compared with the diffusional properties of the whole vesicle measured under high centrifugal force (Huang and Lee, 1973), and also with estimates of lateral diffusion of individual phospholipids within the bilayer (Horwitz et al., 1973).

The pulsed gradient NMR technique for measuring diffusion coefficients employs a simple variation of the two pulse experiment for measuring the $T_2$ relaxation time (McLaughlin et al., 1973). The intensity of the signal from a 90°–$\tau$–180°–$\tau$–observe sequence is measured with and without a field gradient applied during the delay periods, $\tau$. Fourier transformation of the data yields spectral resolution of the resonance permitting the observation of individual species. Because of the field gradient the magnetic field intensity varies through the volume of the sample so that as individual molecules diffuse throughout the sample the individual spins lose their phase coherence causing a loss of signal intensity greater than due to $T_2$ relaxation alone. The ratio of the signal intensity with the gradient on to the intensity with the gradient off is given by

$$I_g/I_0 = \exp[-\tfrac{2}{3}\gamma^2 G^2 D \tau^3] \quad (1)$$

where $G$ is the value of the field gradient, $\tau$ is the delay time, and $\gamma$ is the gyromagnetic ratio. From eq 1, $D$, the diffusion coefficient, can be calculated (James and McDonald, 1973).

## Materials and Methods

L-$\alpha$-Dimyristoyllecithin, deuterium oxide, and calf thymus deoxyribonucleic acid were obtained from Sigma Chemical Co. (St. Louis, Mo.). Liposomes were prepared by sonicating the lecithin in a buffered deuterium oxide solution for 3–6 min with a Branson sonifier operating at maximum power output (Huang, 1969). Tared DNA samples were added to the liposomes subsequent to sonication in experiments where the medium viscosity was altered. A representative sample of sonicated lecithin was applied for chromatography to a Sepharose 4B column at room temperature (26°). The effluent solution was collected on a fraction collector. The phospholipid eluted with a symmetrical peak having the molecular size of the vesicles. No changes in sample turbidity were noted over the course of diffusion measurements. Samples used for NMR analysis were used immediately subsequent to sonication.

NMR spectra were taken on a Varian HR-220 NMR spectrometer equipped with a Fourier transform accessory. Diffusion coefficient measurements were made using the method of James and McDonald (1973). The effective field gradient of 0.4 G/cm was calibrated using quartz distilled degassed water as a standard at 25°. $T_2$ measurements were made using a 180°–$\tau$–90°–$\tau$ pulse sequence as described by McLaughlin et al. (1973). Standard 5-mm sample tubes were used for the relaxation measurements. To avoid modulation artifacts associated with sample spinning, the samples were not spun for the relaxation measurements. Sample temperatures, controlled to ±0.5°, were measured with a thermister thermometer.

$T_2$ data were fitted to an exponential curve using a least-squares routine. Signal intensities are greatly attenuated with the field gradient on. To obtain adequate signal to noise ratios a higher spectrometer gain was used to obtain the data with the field gradient than was used for the $T_2$ measurement.

† From the Department of Biophysics and Physical Biochemistry, University of Pennsylvania, Philadelphia, Pennsylvania 19174. *Received December 26, 1974.* This work was done at the Middle Atlantic Regional NMR Facility (University of Pennsylvania) which is supported by National Institutes of Health Grant RR-542 and was supported in part by National Institutes of Health Grant GM 12202.

[1] Abbreviations used are: NMR, nuclear magnetic resonance; DML, dimyristoyllecithin.

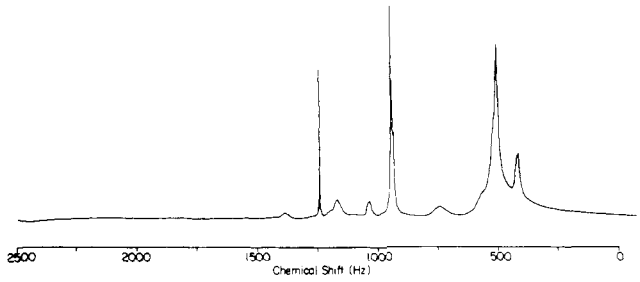


FIGURE 1: The 220-MHz spectrum of sonicated DML, 45 mg/ml, in 10 m*M* sodium phosphate buffer at pD 7.0 and 37°. The peak at 1.25 kHz is from residual HDO. Peak assignments were originally made by Chapman and Morrison (1966).

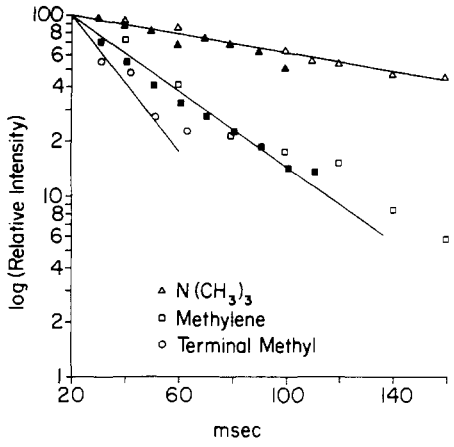


FIGURE 2: $T_2$ relaxation measurements for the major peaks of DML. Experimental conditions are given in Figure 1. Closed and open symbols represent duplicate experiments.

## Results

Figure 1 shows a 220-MHz NMR spectrum of 4% w/w dimyristoyllecithin dispersion in a 10 m*M* sodium phosphate-$D_2O$ buffer at 37°. Spectra were also taken with DML concentrations of 0.3 and 0.03%. No differences in chemical shift, relative intensities, or line widths were observed over this range of concentration. Spectra were also taken for DML in a packed column of Sepharose contained in an NMR tube. There was essentially no difference in line widths between free and Sepharose entrained DML. A slight broadening of all the lines was observed for all the DML lines in a 0.3% w/w calf thymus DNA solution.

$T_2$ relaxation times were measured for the major peaks of DML (Figure 2). Times of 23, 70, and 268 msec were observed for the terminal methyl, methylene, and choline methyl peaks, respectively.

The self-diffusion coefficient for DML in buffer was measured at 37° using the terminal methyl, methylene, and choline methyl resonances. These results appear in Figure 3. A value of $D = 1.25 \times 10^{-6}$ cm$^2$/sec was observed using each resonance. Subsequent measurements were made using only the choline methyl resonances because it afforded a greater signal intensity than the others at long times where the effect of the field gradient is greatest. To ascertain the effect of the macroscopic viscosity on the diffusion of DML, the diffusion coefficient of DML was measured in a packed column of Sepharose equilibrated with $D_2O$. No change in the diffusion coefficient was observed. On the other hand, a diffusion coefficient of $2.19 \times 10^{-7}$ cm$^2$/sec was observed for DML in a 0.3% w/w DNA solution.

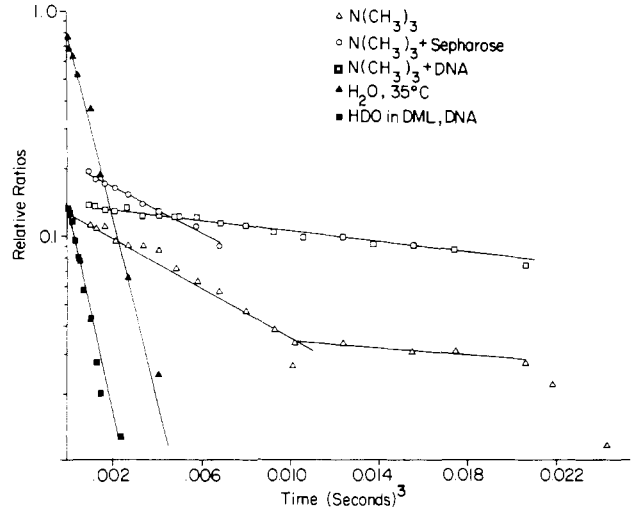


FIGURE 3: Self-diffusion coefficient measurements at 37°: (▲) water at 35°, $D = 1.4 \times 10^{-5}$ cm$^2$/sec; (■) HDO in DML + DNA, $D = 1.4 \times 10^{-5}$ cm$^2$/sec; (△) DML choline methyl, $D = 1.9 \times 10^{-6}$ cm$^2$/sec; (○) DML choline methyl in Sepharose, $D = 1.9 \times 10^{-6}$ cm$^2$/sec; (□) DML choline methyl in DNA, $D = 3.5 \times 10^{-7}$ cm$^2$/sec.

## Discussion

The value for the diffusion coefficient of DML in buffer at 37° was $1.25 \times 10^{-6}$ cm$^2$/sec. Assuming that these liposomes have a diameter of approximately 250 Å (Huang, 1969), Stokes law predicts that such liposomes should diffuse at $1.8 \times 10^{-7}$ cm$^2$/sec in water at 25°. Ultracentrifugation studies on egg lecithin vesicles at 20° show a diffusion rate of $2.03 \times 10^{-7}$ cm$^2$/sec, which is somewhat slower than what we observed for the DML system. Recent light scattering measurements on sphingomyelin show diffusion rates from 2.6 to $4.5 \times 10^{-7}$ cm$^2$/sec (Cooper et al., 1974), and $2.08 \times 10^{-7}$ cm$^2$/sec for phosphatidylcholine-protein complex (Morrisett et al., 1974). By comparison, the values we find for DML are faster by about one order of magnitude. In part, this variation may be accounted for by differences in the respective phospholipid vesicle size.

In principle four mechanisms could contribute to the actual diffusion process. There can be chemical exchange of the individual molecules between the vesicle and the solvent. This may safely be excluded as important because of the low critical micelle concentration of $\simeq 1 \times 10^{-10}$ *M*. Even at fantastically fast exchange rates this contribution to the diffusion rate would be much lower than what we observe. Furthermore it has been shown that intervesicle exchange rate of spin-labeled phospholipids are slow (Kornberg and McConnell, 1971). A second possible mechanism is the rotation of the whole liposome. Another indistinguishable possibility is that molecules could be diffusing within the liposome bilayer. However, both of these may be excluded because of the small field gradient we apply; in a worst case approximation these would contribute less than 10% to the decay rate; so we are forced to conclude that we are observing the diffusion of whole liposomes within the suspension.

Attempts were made to determine how changes in the viscosity would effect the diffusion rate. In the experiment with an NMR tube packed with Sepharose 4B equilibrated with liposomes, the liposome diffusion rate was the same as that observed in buffer. Sepharose has been shown by Huang (1969) to entrain DML liposomes; thus one might expect them to show a smaller diffusion rate than in a free

suspension. It is likely that only a small portion of the DML is entrained and that the retardation one observes by chromatography is observable only when it is magnified by the long column bed. In a highly viscous DNA solution (>10 P) the DML diffusion rate is slowed to only $3.5 \times 10^{-7}$ cm$^2$/sec. This compares with a diffusion rate of $D = 1.8 \times 10^{-8}$ cm$^2$/sec for spin-labeled phosphatidylcholine in vesicles (Devaux and McConnell, 1972) and $D = 1 \times 10^{-8}$ cm$^2$/sec for spin-labeled steroid molecules in dipalmitoyllecithin vesicles (Träuble and Sackmann, 1972). In the DNA solution, the water diffusion rate is undiminished compared with the rate in just buffer. Apparently the DNA forms a network through which water can move unhindered but which entrains the relatively large liposomes.

The decay curve for DML in buffer reproducibly shows a biphasic decay (Figure 3) which could be interpreted in terms of two diffusion processes, one having a fast rate compared with the other. One explanation for this behavior is that the diffusion is partially restricted. At the short times one sees the unrestricted diffusion of DML within a small volume of space. At longer times the DML encounters barriers which impede the migration of the DML from that unit of space. This point deserves further investigation.

## Conclusion

The diffusion of DML in solution is controlled primarily by the translational diffusion of whole liposomes. Translation of individual molecules appears to be a much slower process. One might expect therefore that the diffusion of lipids in biological membranes would be slower than $10^{-7}$ cm$^2$/sec.

## References


Chapman, D., and Morrison, A. (1966), *J. Biol. Chem. 241,* 5044.

Cooper, V. G., Yedgor, S., and Barenholz, Y. (1974), *Biochim. Biophys. Acta 363,* 86.

Devaux, P., and McConnell, H. M. (1972), *J. Am. Chem. Soc. 94,* 4475.

Horwitz, A. F., Klein, M. P., Michaelson, D. M., and Cohler, S. J. (1973), *Ann. N.Y. Acad. Sci. 222,* 468.

Huang, C. (1969), *Biochemistry 8,* 344.

Huang, C., and Lee, L. (1973), *J. Am. Chem. Soc. 95,* 234.

James, T. L., and McDonald, G. G. (1973), *J. Magn. Reson. 11,* 58.

Kornberg, R. G., and McConnell, H. (1971), *Proc. Natl. Acad. Sci. U.S.A. 68,* 2564.

Lee, A. G., Birdsall, N. J. M., and Metcalfe, J. C. (1973), *Biochemistry 12,* 1650.

McLaughlin, A. C., McDonald, G. G., and Leigh, J. S., Jr. (1973), *J. Magn. Reson. 11,* 107.

Morrisett, J. D., Gallagher, J. G., Aune, K. C., and Gotto, A. M., Jr. (1974), *Biochemistry 13,* 4765.

Träuble, H., and Sackmann, E. (1972), *J. Am. Chem. Soc. 94,* 4499.


# Free Energy and the Kinetics of Biochemical Diagrams, Including Active Transport†

Terrell L. Hill

ABSTRACT: In earlier papers on muscle contraction it was found very useful to relate the actual (not standard) free energy levels of the different states in the biochemical diagram of the myosin cross-bridge to the first-order rate constants governing transitions between these states and to the details of the conversion of ATP free energy into mechanical work. This same approach is applied here to other macromolecular biochemical systems, for example, carriers in active transport, and simple enzyme reactions. With the definition of free energy changes between states of a diagram used here (and in the muscle papers), the rate constants of the diagram are first order, the macromolecular transitions are effectively isomeric, the equilibrium constants are dimensionless, the free energy changes are directly related to first-order rate constant ratios, and the ratio of products of forward and backward rate constants around any cycle of the diagram is related to operational free energy changes (e.g., the in vivo free energy of ATP hydrolysis). These general points are illustrated by means of particular arbitrary models, especially transport models. In contrast to the muscle case, the free energy conversion question in other biochemical systems can be handled at the less detailed, complete-cycle level rather than at the elementary transition level. There is a corresponding complete-cycle kinetics, with composite first-order rate constants for the different possible cycles (in both directions). An introductory stochastic treatment of cycle kinetics is included.

A biochemical diagram (see, e.g., Hill, 1968) shows the possible states of a system (usually a macromolecule, or macromolecular complex) as points and represents each inverse pair of possible first-order transitions between two states as a line between the corresponding points.

This paper is concerned primarily with the connections between the free energies of the states of a diagram and the first-order rate constants associated with the transitions or lines in the diagram. The discussion applies to biochemical diagrams generally but free energy transducing systems are of primary interest.

Actually, this subject was introduced, from the present

† From the Laboratory of Molecular Biology, National Institute of Arthritis, Metabolism, and Digestive Diseases, National Institutes of Health, Bethesda, Maryland 20014. *Received December 6, 1974.*